

ANALYTICAL-NUMERICAL SOLUTION OF STATIC PROBLEMS FOR NONCIRCULAR CYLINDRICAL SHELLS OF VARIABLE THICKNESS

E. A. Storozhuk* and A. V. Yatsura**

An analytical-numerical method of solving boundary-value static problems for transversally isotropic infinitely long noncircular cylindrical shells of variable thickness is formulated and developed. The system of basic equations is derived using the relations of the refined theory of deep shells with low shear stiffness. Expressions for internal power factors and generalized displacements of closed and open cylindrical shells with arbitrary cross-section acted upon by surface and linear forces are presented. The integrals appearing in these expressions are calculated with the method of trapezoids. The numerical results for a closed shell of elliptic cross-section under uniform internal pressure presented in the form of tables and plots are analyzed

Keywords: long cylindrical shell, noncircular cross-section, analytical-numerical solution, variable thickness, deformation of transverse shear, static load

Introduction. Noncircular cylindrical shells, which are used in different fields of technology, industrial and civil engineering, in a number of cases are more strong, stable and light in comparison with shells of circular cross-section.

Due to variability in radius of curvature of cross-sections, the solution of boundary-value problems for noncircular shells involves severe mathematical difficulties. The exact analytical solutions of the given problems have been obtained only for an infinitely long cylindrical shell with oval cross-section [12] and cross-section whose curvature varies by the quadratic law [4]. Because of this, in analyzing noncircular shells, numerical, approximate analytical, and experimental methods are widely used that makes it possible to study the stress-strain state (SSS), stability, and vibrations of oval and elliptic cylindrical shells of constant and variable thickness [1–3, 7, 10, 11, 13–18].

In numerical solving the boundary-value problems for infinitely long closed cylindrical shells with a noncircular cross-section, we meet with so-called locking. The computational phenomenon of membrane locking has been demonstrated by examples of the variational-difference and finite-element methods presented in [2] and [7], respectively. From the point of view of locking, two-dimensional deformation of a noncircular cylindrical shell with fixed ends presents the simpler problem due to decrease in bends as a result of reinforcing action of ends.

In what follows, we will formulate the statement of the static problems for an infinitely long noncircular cylindrical shell of variable thickness with allowance for transversal shear strains and develop the analytical-numerical procedure, free of membrane and shear locking, for numerical solving of the above class of problems. We will consider, as an example, a closed elliptical shell under uniform normal pressure.

1. Problem statement. Basic relations. Let us consider an infinitely long cylindrical shell of arbitrary cross-section made of a transversally isotropic material and acted upon by surface and linear forces. Assume that the directrix of the shell cross-section varies smoothly while the shell thickness h along the generatrix is constant and continuously varies along the directrix. The load applied to the shell is uniformly distributed along the generatrix. Under such conditions, the displacements, strains, and stresses in each cross-section will be the same while all searched values will vary along the directrix only.

S. P. Timoshenko Institute of Mechanics, National Academy of Sciences of Ukraine, 3 Nesterova St., Kyiv, Ukraine 03057, e-mail: *stevan@ukr.net, **andriy.yatsura.88@gmail.com. Translated from *Prikladnaya Mekhanika*, Vol. 53, No. 3, pp. 91–103, May–June, 2017. Original article submitted February 28, 2016.

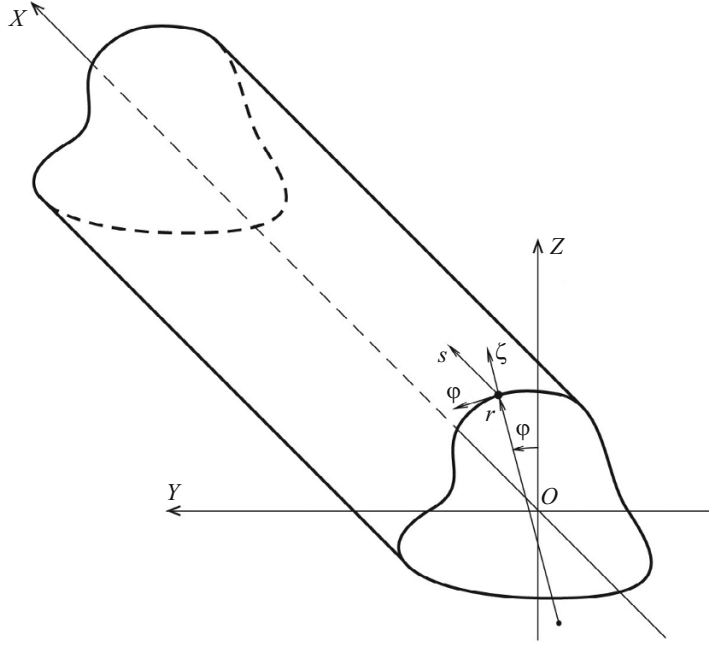


Fig. 1

To describe the shell, we will use a curvilinear orthogonal coordinate system (s, φ, ζ) aligned with the lines of principal curvature (Fig. 1). Here s and ζ are the lengths of the generatrix and normal to the coordinate surface ($\zeta=0$), φ is the angle between the normal to the coordinate surface and vertical axis.

We will present the coordinate surface of the shell in the global Cartesian coordinate system (X, Y, Z) , whose OX -axis is parallel to the generatrix (Fig. 1). Then the cross-section plane (Y, Z) in a parametric form will be described as $Y = Y(\varphi)$, $Z = Z(\varphi)$, $\varphi_1 \leq \varphi \leq \varphi_2$.

In studying the SSS of long nonthin cylindrical shells with noncircular cross-section, the equations of the refined shell theory, which is based on the straight-line hypothesis (the transverse shear strains are taken into account), are considered as initial ones. In this case, kinematic equations take the following form [1]:

$$\varepsilon = \frac{du}{rd\varphi} + \frac{w}{r}, \quad \gamma = \vartheta + \frac{dw}{rd\varphi} - \frac{1}{r}u, \quad \mu = \frac{d\vartheta}{rd\varphi}, \quad (1.1)$$

where ε, γ, μ are the strain components of the shell; u, w are the tangential displacement and bending of the shell mid-surface; ϑ is the angle of rotation of the normal; r is the cross-sectional radius curvature.

In accordance with Hooke's law, the internal forces and moment are related to the strain components as follows:

$$N = D_N \varepsilon, \quad D_N = \frac{Eh}{1-\nu^2}, \quad Q = D_Q \gamma, \quad D_Q = kG_{\varphi\zeta} h, \\ M = D_M \mu, \quad D_M = D_N h^2 / 12, \quad (1.2)$$

where N and Q are the tangential and shearing forces; M is the bending moment; D_N, D_M, D_Q are the stiffness characteristics of the shell; E and ν are the elastic modulus and Poisson's ratio in the isotropy plane; $G_{\varphi\zeta}$ is the shear modulus in the cross-sectional plane; k is a coefficient depending on how the shear is distributed across the thickness and mean value of the shear is determined.

The equilibrium equations are

$$\frac{dN}{rd\varphi} + \frac{1}{r}Q + q_\varphi = 0, \quad \frac{dQ}{rd\varphi} - \frac{1}{r}N + q_\zeta = 0, \quad \frac{dM}{rd\varphi} - Q = 0, \quad (1.3)$$

where q_φ, q_ζ are the components of the surface load.

2. General Solution for a Noncircular Cylindrical Shell of Variable Thickness. From the two first equations in (1.3), we obtain the following equation to determine the transverse force:

$$\frac{d^2 Q}{d\varphi^2} + Q = -r q_\varphi - \frac{d(r q_\zeta)}{d\varphi}. \quad (2.1)$$

The characteristic equation $k^2 + 1 = 0$ of the associated homogeneous equation has roots $k_{1,2} = \pm i$. Because of this, the function $Q^* = C_1 \cos \varphi + C_2 \sin \varphi$ yields the general solution of a homogeneous equation. The partial solution Q^{**} of the inhomogeneous equation (2.1) should be found with the method of variation of arbitrary constants. In this case, we arrive at the general solution of Eq. (2.1) in the form

$$Q = C_1 \cos \varphi + C_2 \sin \varphi + \cos \varphi \int_0^\varphi q_1 dx - \sin \varphi \int_0^\varphi q_2 dx + (r q_\zeta)|_0 \sin \varphi, \quad (2.2)$$

where $q_1 = r(q_\varphi \sin x - q_\zeta \cos x)$, $q_2 = r(q_\varphi \cos x + q_\zeta \sin x)$.

The tangential force can be found from the second equilibrium equation in (2.2):

$$N = \frac{dQ}{d\varphi} + r q_\zeta = -C_1 \sin \varphi + C_2 \cos \varphi - \sin \varphi \int_0^\varphi q_1 dx - \cos \varphi \int_0^\varphi q_2 dx + (r q_\zeta)|_0 \cos \varphi. \quad (2.3)$$

From the third equilibrium equation in (1.3), we determine the moment

$$M = \int_0^\varphi r Q dx + C_3 = M^* + C_3, \quad M^* = \int_0^\varphi r Q dx. \quad (2.4)$$

Using the kinematic relation for the bending strain (1.1), whose value ($\mu = M / D_M$) is calculated with (1.2), we arrive at a formula for the angle of rotation of the normal:

$$\vartheta = \int_0^\varphi r \mu dx + C_4 = \int_0^\varphi \frac{r M dx}{D_M} + C_4 = \int_0^\varphi \frac{r M^* dx}{D_M} + C_3 \int_0^\varphi \frac{r dx}{D_M} + C_4. \quad (2.5)$$

Then the tangential displacement follows from the second-order linear inhomogeneous differential equation with constant coefficients

$$\frac{d^2 u}{d\varphi^2} + u = \frac{d}{d\varphi} (r \varepsilon) + r(\vartheta - \gamma), \quad (2.6)$$

where $\varepsilon = N / D_N$, $\gamma = Q / D_Q$.

The general solution of equation (2.6) is

$$u = C_5 \cos \varphi + C_6 \sin \varphi + \cos \varphi \int_0^\varphi f_1 dx + \sin \varphi \int_0^\varphi f_2 dx - r \varepsilon|_0 \sin \varphi, \quad (2.7)$$

where

$$f_1 = r[\varepsilon \cos x - (\vartheta - \gamma) \sin x] \quad f_2 = r[\varepsilon \sin x + (\vartheta - \gamma) \cos x]. \quad (2.8)$$

With $w = rN / D_N - u'_\varphi$, we obtain an expression for the deflection:

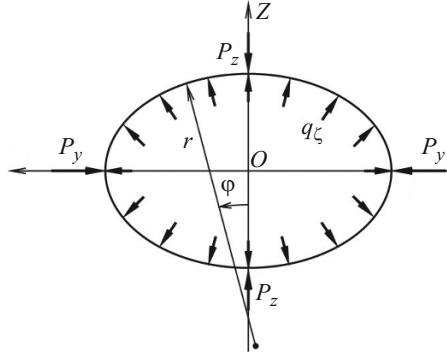


Fig. 2

$$w = C_5 \sin \varphi - C_6 \cos \varphi + \sin \varphi \int_0^\varphi f_1 dx - \cos \varphi \int_0^\varphi f_2 dx + r\varepsilon|_0 \cos \varphi. \quad (2.9)$$

In solving specific problems, the integration constants (C_1, C_2, \dots, C_6) are determined from the appropriate boundary conditions.

3. Closed Infinitely Long Cylindrical Shell with Noncircular Cross-Section. Assume that the cross-section of a long cylindrical shell closed along the directrix ($-\pi \leq \varphi \leq \pi$) has two mutually perpendicular OY - and OZ -axes of symmetry. The shell is acted upon by two pairs of antipodal transverse forces $P_y = \text{const}$ and $P_z = \text{const}$ uniformly distributed along the generatrices and by normal surface forces $q_\zeta = q_\zeta(\varphi)$ applied symmetrically with respect to the XOY - and XOZ -planes (Fig. 2).

Since the cross-sectional geometry and force distribution are symmetrical, we will consider a quarter ($0 \leq \varphi \leq \pi/2$) of the shell cross-section as a design model and specify the following boundary conditions at the points $\varphi = 0$ and $\varphi = \pi/2$:

$$u(0) = \vartheta(0) = 0, \quad Q(0) = \frac{P_z}{2}, \quad u\left(\frac{\pi}{2}\right) = \vartheta\left(\frac{\pi}{2}\right) = 0, \quad Q\left(\frac{\pi}{2}\right) = -\frac{P_y}{2}. \quad (3.1)$$

The stress-strain state of the shell is described by the system of equations (1.1)–(1.3), whose general solution is presented in Sec. 2. The integration constants are determined using the boundary conditions (3.1).

At first, we define the integration constants C_1 and C_2 from the boundary conditions for transverse forces $Q(0) = P_z/2$ and $Q(\pi/2) = -P_y/2$:

$$C_1 = \frac{P_z}{2}, \quad C_2 = \int_0^{\pi/2} r q_\zeta \sin x dx - (r q_\zeta)|_0 - \frac{P_y}{2}. \quad (3.2)$$

For the internal forces, which satisfy the prescribed boundary conditions (3.1), we have:

$$Q = \frac{P_z}{2} \cos \varphi - \frac{P_y}{2} \sin \varphi - \cos \varphi \int_0^\varphi r q_\zeta \cos x dx + \sin \varphi \int_\varphi^{\pi/2} r q_\zeta \sin x dx,$$

$$N = -\frac{P_z}{2} \sin \varphi - \frac{P_y}{2} \cos \varphi + \sin \varphi \int_0^\varphi r q_\zeta \cos x dx + \cos \varphi \int_\varphi^{\pi/2} r q_\zeta \sin x dx. \quad (3.3)$$

Next, using boundary conditions $\vartheta(0) = 0$ and $\vartheta(\pi/2) = 0$, we find the constants C_3 and C_4 :

$$C_3 = -\frac{1}{L} \int_0^{\pi/2} \frac{rM^*}{D_M} dx, \quad L = \int_0^{\pi/2} \frac{rdx}{D_M}, \quad C_4 = 0. \quad (3.4)$$

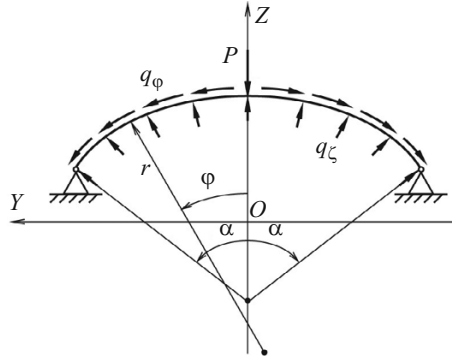


Fig. 3

Then, using formulas (2.4) and (2.5), we define the moment and angle of rotation of the normal:

$$M = M^* - \frac{1}{L} \int_0^{\pi/2} \frac{rM^*}{D_M} dx, \quad \vartheta = \int_0^{\varphi} \frac{rM}{D_M} dx. \quad (3.5)$$

From the boundary conditions for the tangential displacement $u(0) = 0$ and $u(\pi/2) = 0$, we obtain the values of the constants C_5 and C_6 :

$$C_5 = 0, \quad C_6 = \frac{rN}{D_N} \Big|_0^{\pi/2} - \int_0^{\pi/2} f_2 dx. \quad (3.6)$$

Substituting the expressions for C_5 and C_6 into (2.7) and (2.9) and performing some transformations, we obtain formulas for the tangential displacement and deflection:

$$u = \cos \varphi \int_0^{\varphi} f_1 dx - \sin \varphi \int_{\varphi}^{\pi/2} f_2 dx,$$

$$w = \sin \varphi \int_0^{\varphi} f_1 dx + \cos \varphi \int_{\varphi}^{\pi/2} f_2 dx. \quad (3.7)$$

4. Open Long Cylindrical Shell with Noncircular Cross-Section and Hinged Longitudinal Edges. Let us study the strain state of an open (along a directrix $-\alpha \leq \varphi \leq \alpha$) long cylindrical shell with arbitrary cross-section and hinged longitudinal edges ($\varphi = \pm \alpha$). The shell is subject to normal $q_\zeta = q_\zeta(\varphi)$ and tangential $q_\varphi = q_\varphi(\varphi)$ surface forces as well as a transverse force $P = \text{const}$ applied at the apex (Fig. 3) and uniformly distributed along the generatrix.

The cross-section and load are symmetrical with respect to the vertical plane XOZ . This makes it possible to consider only half ($0 \leq \varphi \leq \alpha$) the shell. Let $u = w = M = 0$ at the edge $\varphi = \alpha$ and $u = \vartheta = 0$ and $Q = P/2$ on the edge $\varphi = 0$.

Determining the integration constant $C_1 = P/2$ from the boundary condition $Q(0) = P/2$, we represent the internal forces (2.2) and (2.3) as follows:

$$Q = C_2 \sin \varphi + Q_1, \quad N = C_2 \cos \varphi + N_1, \quad (4.1)$$

where C_2 is the unknown constant of integration;

$$Q_1 = \frac{P}{2} \cos \varphi + \cos \varphi \int_0^{\varphi} q_1 dx - \sin \varphi \int_0^{\varphi} q_2 dx + (rq_\zeta)|_0 \sin \varphi,$$

$$N_1 = -\frac{P}{2} \sin \varphi - \sin \varphi \int_0^\varphi q_1 dx - \cos \varphi \int_0^\varphi q_2 dx + (rq_\zeta)|_0 \cos \varphi. \quad (4.2)$$

Substituting the relation for transverse force (4.1) into the expression for moment (2.4), we arrive at the formula

$$M = C_2 l_0 + M_0 + C_3, \quad (4.3)$$

where

$$l_0 = \int_0^\varphi r \sin x dx, \quad M_0 = \int_0^\varphi r Q_1 dx. \quad (4.4)$$

Let us express the integration constant C_3 that appears in (4.3) in terms of the constant C_2 using the boundary condition $M(\alpha) = 0$:

$$C_3 = -C_2 l_0(\alpha) - M_0(\alpha). \quad (4.5)$$

Then the expression for the moment becomes:

$$M = C_2 l_1 + M_1, \quad (4.6)$$

where

$$M_1 = M_0 - M_0(\alpha), \quad l_1 = l_0 - l_0(\alpha). \quad (4.7)$$

In accordance with the boundary condition $\vartheta(0) = 0$, the constant C_4 appearing in (2.5) is equal to zero.

With (2.5) and (4.6), the expression for the angle of rotation of the normal becomes:

$$\vartheta = C_2 l_2 + \vartheta_1, \quad (4.8)$$

where

$$\vartheta_1 = \int_0^\varphi \frac{r M_1}{D_M} dx, \quad l_2 = \int_0^\varphi \frac{r l_1}{D_M} dx. \quad (4.9)$$

The boundary condition for the tangential displacement at the shell apex ($u(0) = 0$) is satisfied if $C_5 = 0$.

Satisfying the boundary conditions at the longitudinal edge $\varphi = \alpha$ ($u(\alpha) = 0$ and $w(\alpha) = 0$), we arrive at a system of equations for the remaining constants C_2 and C_6 :

$$\begin{cases} C_6 \sin \alpha + \cos \alpha \int_0^\alpha f_1 dx + \sin \alpha \int_0^\alpha f_2 dx - \frac{rN}{D_N} \Big|_0 \sin \alpha = 0, \\ -C_6 \cos \alpha + \sin \alpha \int_0^\alpha f_1 dx - \cos \alpha \int_0^\alpha f_2 dx + \frac{rN}{D_N} \Big|_0 \cos \alpha = 0. \end{cases} \quad (4.10)$$

Solving this system, we obtain:

$$C_6 = \frac{rN}{D_N} \Big|_0 - \int_0^\alpha f_2 dx, \quad \int_0^\alpha f_1 dx = 0. \quad (4.11)$$

At first, we determine the integration constant C_2 from the equation $\int_0^\alpha f_1 dx = 0$:

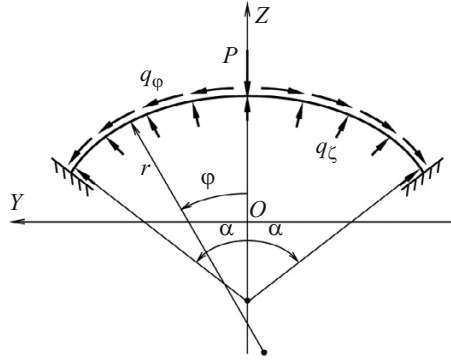


Fig. 4

$$C_2 = - \frac{\int_0^\alpha r \left[\frac{N_1 \cos x}{D_N} - \left(\vartheta_1 - \frac{Q_1}{D_Q} \right) \sin x \right] dx}{\int_0^\alpha r \left[\frac{\cos^2 x}{D_N} - \left(l_2 - \frac{\sin x}{D_Q} \right) \sin x \right] dx}. \quad (4.12)$$

Next, we find values N, Q, M, ϑ , and C_6 by formulas (4.1), (4.6), (4.8), and (4.11).

Using values of the integration constants, we reduce Eqs. (2.7) and (2.9) for the shell displacements to the following form:

$$\begin{aligned} u &= \cos \varphi \int_0^\varphi f_1 dx - \sin \varphi \int_0^\alpha f_2 dx, \\ w &= \sin \varphi \int_0^\varphi f_1 dx + \cos \varphi \int_0^\alpha f_2 dx. \end{aligned} \quad (4.13)$$

5. Open Long Noncircular Cylindrical Shell with Clamped Longitudinal Edges. Consider an infinitely long cylindrical shell, open along the directrix, with a noncircular cross-section. The longitudinal edges of the shell are clamped. The shell is made of a transversely isotropic material and subject to surface $q_\zeta = q_\zeta(\varphi)$ and $q_\varphi = q_\varphi(\varphi)$ and linear forces $P = \text{const}$ (Fig. 4).

Taking into account the geometrical and force symmetry with respect to the vertical plane XOZ , we will restrict our calculations to the half the shell ($0 \leq \varphi \leq \alpha$). Assume that the edge $\varphi = \alpha$ is clamped ($u = w = \vartheta = 0$), while the edge $\varphi = 0$ is under mixed boundary conditions ($u = \vartheta = 0$ and $Q = P/2$).

It should be noted that initial equations (equilibrium, constitutive, and kinematic) are the same as in the previous problem. Because of this, in calculating the internal forces N, Q , moment M , angle of rotation of the normal ϑ , and displacements u, w of the shell, we can use the formulas presented in Sec. 4. The differences are held only in determining the integration constant C_3 (4.5) and components M_1, l_1 (4.7) defined as follows:

(i) the angle of rotation of the normal is determined by substituting (4.3) into (2.5):

$$\vartheta = C_2 \int_0^\varphi \frac{rl_0}{D_M} dx + \int_0^\varphi \frac{rM_0}{D_M} dx + C_3 \int_0^\varphi \frac{rdx}{D_M} + C_4. \quad (5.1)$$

(ii) the constant $C_4 = 0$ is determined from the condition $\vartheta(0) = 0$ and the constant C_3 from the condition $\vartheta(\alpha) = 0$:

$$C_3 = - \frac{C_2}{L} \int_0^\alpha \frac{rl_0}{D_M} dx - \frac{1}{L} \int_0^\alpha \frac{rM_0}{D_M} dx, \quad L = \int_0^\alpha \frac{rdx}{D_M}. \quad (5.2)$$

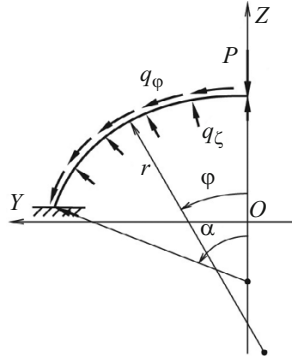


Fig. 5

(iii) considering (5.2), the components of the moment appearing in (4.6) take the form

$$M_1 = M_0 - \frac{1}{L} \int_0^\alpha \frac{rM_0}{D_M} dx, \quad l_1 = l_0 - \frac{1}{L} \int_0^\alpha \frac{rl_0}{D_M} dx. \quad (5.3)$$

6. Long Cylindrical Panel with Noncircular Cross-Section and One Longitudinal Edge Being Clamped. Consider an open infinitely long cylindrical shell with arbitrary cross-section whose longitudinal edge $\varphi = \alpha$ is clamped while the edge $\varphi = 0$ is subject to a shearing force $P = \text{const}$. Moreover, the panel is subject to normal $q_\zeta = q_\zeta(\varphi)$ and tangential $q_\varphi = q_\varphi(\varphi)$ surface forces (Fig. 5).

The general solution of the problem is described by Eqs. (2.2)–(2.5), (2.7), (2.9). The integration constants are determined from the following boundary conditions:

$$Q(0) = P, \quad N(0) = M(0) = 0, \quad u(\alpha) = w(\alpha) = \vartheta(\alpha) = 0. \quad (6.1)$$

Substituting solutions (2.2)–(2.5), (2.7), (2.9) into (6.1), we arrive at a system of six equations:

$$\begin{cases} C_1 - P = 0, \\ C_2 + (rq_\zeta)|_0 = 0, \\ C_3 = 0, \\ C_4 + \int_0^\alpha \frac{rM}{D_M} dx = 0, \\ C_5 \cos \alpha + C_6 \sin \alpha + \cos \alpha \int_0^\alpha f_1 dx + \sin \alpha \int_0^\alpha f_2 dx - \frac{rN}{D_N} \Big|_0 \sin \alpha = 0, \\ C_5 \sin \alpha - C_6 \cos \alpha + \sin \alpha \int_0^\alpha f_1 dx - \cos \alpha \int_0^\alpha f_2 dx + \frac{rN}{D_N} \Big|_0 \cos \alpha = 0. \end{cases} \quad (6.2)$$

The constants $C_1 - C_6$ can be determined from (6.2):

$$C_1 = P, \quad C_2 = -(rq_\zeta)|_0, \quad C_3 = 0, \quad C_4 = -\int_0^\alpha \frac{rM}{D_M} dx, \quad C_5 = -\int_0^\alpha f_1 dx, \quad C_6 = \frac{rN}{D_N} \Big|_0 - \int_0^\alpha f_2 dx. \quad (6.3)$$

As a result, we obtain the following expressions for the internal force factors and generalized displacements of the panel:

$$Q = P \cos \varphi + \cos \varphi \int_0^\varphi q_1 dx - \sin \varphi \int_0^\varphi q_2 dx, \quad N = -P \sin \varphi - \sin \varphi \int_0^\varphi q_1 dx - \cos \varphi \int_0^\varphi q_2 dx,$$

TABLE 1

SSS	φ	$\tilde{\zeta}$	Analytical-numerical solution					Exact solution
			$n = 10$	$n = 25$	$n = 50$	$n = 100$	$n = 200$	
$\tilde{\sigma}$	0	0.5	108.056	109.689	109.922	109.981	109.995	110
		-0.5	-92.122	-93.699	-93.925	-93.981	-93.995	-94
	$\pi/2$	0.5	-124.470	-125.388	-125.939	-125.985	-125.996	-126
		-0.5	148.453	149.354	149.938	149.984	149.996	150
\tilde{w}	0	0	3.99900	4.09961	4.11413	4.11776	4.11867	4.11898
	$\pi/2$	0	-2.84891	-2.87974	-2.89762	-2.89915	-2.89954	-2.89966
$\Delta_{\max}, \%$			2.00	0.69	0.12	0.03	0.008	0

$$M = \int_0^{\varphi} rQ dx, \quad \vartheta = -\int_{\varphi}^{\alpha} \frac{rM}{D_M} dx,$$

$$u = -\cos \varphi \int_{\varphi}^{\alpha} f_1 dx - \sin \varphi \int_{\varphi}^{\alpha} f_2 dx, \quad w = -\sin \varphi \int_{\varphi}^{\alpha} f_1 dx + \cos \varphi \int_{\varphi}^{\alpha} f_2 dx. \quad (6.4)$$

7. Evaluation of the Integrals Appearing in the Expressions for Internal Forces and Generalized Displacements.

Because the integrands that appear in the formulas for internal forces, bending moment, angle of rotation of the normal, tangential displacement, and shell deflection are continuous, the integrals in these formulas exist, but the primitive functions for the most of the cross-sections of the cylindrical shell cannot be expressed in terms of elementary functions. For this reason, these integrals should be evaluated numerically with the trapezoidal rule:

$$\int_a^b g(x) dx \approx \Delta x \left[\frac{g(a) + g(b)}{2} + g(x_1) + g(x_2) + \dots + g(x_{n-1}) \right], \quad (7.1)$$

where $x_i = a + i\Delta x$ are the integration nodes that divide the segment $[a, b]$ into n equal parts of length $\Delta x = (b - a) / n$.

Note that the integrand in the trapezoidal formula can be defined either analytically or by a table collecting its values at the integration nodes.

8. Validation of the Analytical-Numerical Approach. To estimate the efficiency of the method developed, we will solve a number of test problems and compare the results obtained with the exact solution. As an example, we will consider the boundary-value problem on the SSS of a closed infinitely long cylindrical shell with oval cross-section. The shell is acted upon by uniform internal pressure $q = \text{const}$.

Let us assume that the shell cross-section has two symmetry axes and is described parametrically as

$$Y = r_0 \left[\left(1 + \frac{\xi}{2} \right) \sin \varphi + \frac{\xi}{6} \sin 3\varphi \right], \quad Z = r_0 \left[\left(1 - \frac{\xi}{2} \right) \cos \varphi + \frac{\xi}{6} \cos 3\varphi \right],$$

$$r_0 = \frac{a+b}{2}, \quad \xi = 3 \frac{a-b}{a+b}, \quad -\pi \leq \varphi \leq \pi, \quad (8.1)$$

TABLE 2

K	SSS	φ	$\tilde{\zeta}$	a / b					
				1.0	1.2	1.4	1.6	1.8	2.0
1; 2	$\tilde{\sigma}$	0	0.5	10	61	100	130	155	175
			-0.5	10	-43	-83	-115	-141	-161
		$\pi/2$	0.5	10	-46	-97	-142	-182	-219
			-0.5	10	68	120	166	208	245
1	\tilde{w}	0	0.0	0.0091	0.6831	1.3210	1.9103	2.4485	2.9380
		$\pi/2$	0.0	0.0091	-0.5568	-0.9409	-1.2018	-1.3783	-1.4960
2	\tilde{w}	0	0.0	0.0091	0.3716	0.7201	1.0448	1.3432	1.6157
		$\pi/2$	0.0	0.0091	-0.2876	-0.4820	-0.6084	-0.6893	-0.7395

where a and b are the major and minor semi-axes of the cross-section.

The curvature radius of the oval is calculated by

$$r = r_0 (1 + \xi \cos 2\varphi). \quad (8.2)$$

The input data in the case of the constant thickness h are: $r_0 / h = 10$, $a / b = 1.5$, $E = 38.4$ GHz, $G_{\varphi\zeta} = 0.2$ GPa, $\nu = 0.1933$, $k = 5/6$.

Table 1 summarizes values of the dimensionless deflections $\tilde{w} = wE_0 / hq$ ($E_0 = 10$ MPa) and stresses $\tilde{\sigma} = \sigma / q$ ($\sigma = N / h + M\zeta / h^3$) on the outside ($\tilde{\zeta} = \zeta / h = 0.5$) and inside ($\tilde{\zeta} = -0.5$) shell surfaces at two points of the cross-sectional contour (at the ends of the minor and major semi-axes). The data are obtained with the method developed (analytical-numerical solution) for the number n of parts into which the integration segment $[0, \pi/2]$ is divided. The results of the analytical (exact) solution [12] are presented in the same table.

Analysis of Table 1 reveals that the maximum difference (Δ_{\max}) between the exact solution and the analytical-numerical solutions obtained with the integration interval divided into 10, 25, 50, 100, 200 parts does not exceed 2.00, 0.69, 0.12, 0.03, 0.008%, respectively.

Thus, the analytical-numerical method developed for solving boundary-value problems for infinitely long noncircular cylindrical shells eliminates entirely the adverse locking effect. This increases considerably the accuracy of solutions.

9. Numerical Results and Their Analysis.

9.1. Noncircular Cylindrical Shell of Constant Thickness. Consider an infinitely long closed cylindrical shell of constant thickness with elliptic cross-section. The shell is acted upon by uniform internal pressure q .

The cross-section of the coordinate surface of the shell is defined parametrically as

$$Y = \frac{a^2 \sin \varphi}{(a^2 \sin^2 \varphi + b^2 \cos^2 \varphi)^{1/2}}, \quad Z = \frac{b^2 \cos \varphi}{(a^2 \sin^2 \varphi + b^2 \cos^2 \varphi)^{1/2}},$$

where a and b are the ellipse semi-axes.

The curvature radius of the ellipse is calculated as follows:

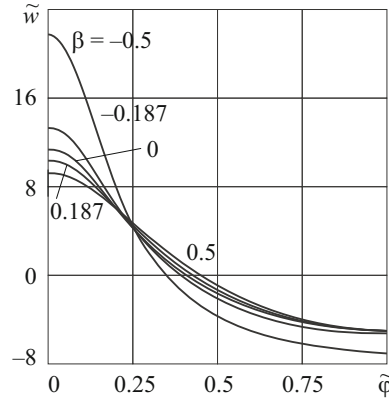


Fig. 6

$$r = \frac{a^2 b^2}{(a^2 \sin^2 \varphi + b^2 \cos^2 \varphi)^{3/2}}$$

The input data are: $r_0 / h = 10$, $E = 38.4$ GPa, $G_{\varphi\zeta} = 0.005E$, $\nu = 0.3$, $k = 5/6$.

Values of the dimensionless deflections $\tilde{w} = wE / 10^4 hq$ and stresses $\tilde{\sigma} = \sigma / q$ on the outside ($\tilde{\zeta} = 0.5$) and inside ($\tilde{\zeta} = -0.5$) surfaces of the shell at the ends of minor and major semi-axes ($\varphi = 0$ and $\varphi = \pi/2$) are collected in Table 2. The data are obtained for a number of aspect ratios ($a/b = 1.0, 1.2, 1.4, 1.6, 1.8, 2.0$) and two values of K : $K = 1$ (Timoshenko's model) and $K = 2$ (Kirchhoff-Love model).

An analysis of the results obtained reveals that the deflections in closed elliptical shells subjected to uniform internal pressure are maximum at the end ($\varphi = 0$) of the minor semi-axis. Allowing for the strains of transverse shear ($K = 1$) results in an increase of maximum deflections compared with the Kirchhoff-Love model ($K = 2$). At $a/b = 1.0, 1.2, 1.4, 1.6, 1.8, 2.0$, the maximum deflection increases by 0, 84, 83, 83, 82, 82%, respectively.

The shell with elliptical cross-section acted upon by internal pressure at the above aspect ratios tends to the circular form that results in occurrence of deflections with dissimilar signs at the points $\varphi = 0$ and $\varphi = \pi/2$.

The results obtained show that stresses in closed shells are maximum at the end of the major semi-axis on the inside surface of the shell. The stresses obtained with both models ($K = 1$ and 2) are similar.

The maximum values of all the SSS components considerably increase with deviation of the cross-section from circular shape (with increase in a/b). Thus, in calculations with allowance for transverse shear strains at $a/b = 2.0$, the maximum stresses increase by a factor of 24.5, whereas the maximum deflection by a factor of 323.

9.2. Noncircular Cylindrical Shell with Variable Thickness. Consider a closed elliptical cylindrical shell with thickness varying along the directrix. The shell is subject to uniform normal pressure $q = \text{const}$. The shell thickness varies as $h = h_0(1 + \beta \cos 2\varphi)$ so that the weight of the shell remains unchanged with variation in the parameter β [1].

Let us study how the variation in the shell thickness influences the distribution of the deflection and stresses along the directrix while its weight remains constant if $r_0 / h_0 = 15$, $a/b = 2$, $E = 38.4$ GPa, $G_{\varphi\zeta} = 0.005E$, $\nu = 0.3$, $k = 5/6$, $\beta = 0, \pm 0.187, \pm 0.3, \pm 0.5$.

Figures 6–8 demonstrate the distribution of the dimensionless deflections $\tilde{w} = wE / 10^4 h_0 q$ and stresses on the outside ($\tilde{\sigma}^+$) and inside ($\tilde{\sigma}^-$) surfaces of the shell along the directrix ($0 \leq \tilde{\varphi} \leq 1$, $\tilde{\varphi} = 2\varphi / \pi$) depending on the thickness ($\beta = 0, \pm 0.187, \pm 0.5$).

Table 3 summarizes maximum relative stresses $\tilde{\sigma}_{\max}$ and deflections \tilde{w}_{\max} for a number of values of the coefficient β .

The data presented in Fig. 6 and Table 3 show that the deflections are maximum for all values of β at the end ($\varphi = 0$) of the major semi-axis, i.e., the maximum deflection increases with the thickness in the vicinity of the apex of the minor axis of the ellipse and at $\beta = -0.5$ exceeds the same value for the shell with constant thickness ($\beta = 0$) by a factor of 1.94. Increase in the thickness in this region ($\beta = 0.187, 0.3, 0.5$) results in a negligible decrease of the maximum deflection.

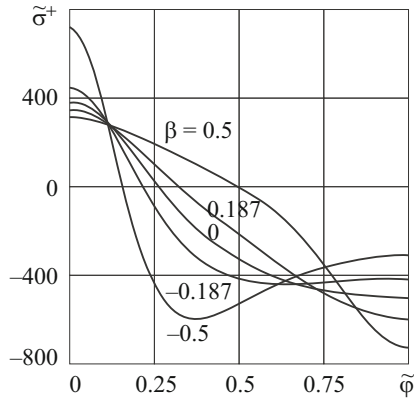


Fig. 7

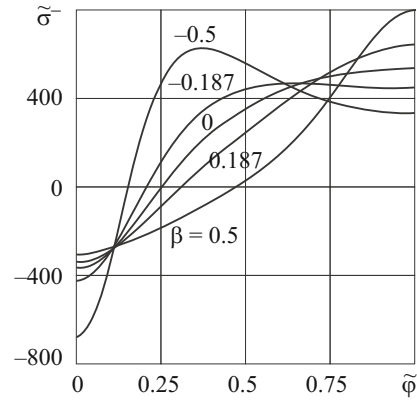


Fig. 8

TABLE 3

SSS	β						
	-0.5	-0.3	-0.187	0	0.187	0.3	0.5
$\tilde{\sigma}_{\max}$	721	513	450	542	648	713	807
\tilde{w}_{\max}	21.623	15.001	13.059	11.137	10.074	9.638	8.967

As is seen from Figs. 7 and 8 and Table 3, the stresses peak on the inside surface of the shell in the section $\varphi = \pi/2$ at $\beta = 0, 0.187, 0.3, 0.5$, on the outside surface in the section $\varphi = 0$ at $\beta = -0.3, -0.5$, on the inside surface in the section $\varphi = \pi/2$ and the outside surface in the section $\varphi = 0$ at $\beta = -0.187$, i.e., $\tilde{\sigma}_{\max} = \tilde{\sigma}^-(\pi/2) = \tilde{\sigma}^+(0) = 450$. Therefore, at $\beta = 0.187, \pm 0.3, \pm 0.5$, the stresses are maximum in sections with minimum thickness.

Applying the minimax criterion [9], which minimizes the maximum stress, to the data in Table 3, we can conclude that the thickness variation law (9.3) is optimal at $\beta = -0.187$.

Considering the shell thickness at $\beta = -0.187$ as a reference point, we see that the maximum stress increases with decrease in the thickness in the vicinity of the major axis ($\beta = 0, 0.187, 0.3, 0.5$) or in the vicinity of the minor semi-axis ($\beta = -0.3, -0.5$) and exceeds the stress for the shell with optimal thickness by 60% at $\beta = -0.5$ and by 79% at $\beta = 0.5$, the weight of the shell remaining constant.

Thus, by varying the shell thickness, it is possible to control the distribution of the SSS components along the directrix with the weight being unchanged.

Conclusions. We have developed an analytical-numerical method to solve linear elastic static problems for transversally isotropic long cylindrical shells with noncircular cross-section. The method, based on analytical and numerical integration, takes into account transverse-shear strains, is free of locking, and ensures high accuracy of the results. Using the method, we have studied how the aspect ratio of the cross-section, the transverse-shear strains, and thickness influence the stress-strain state of a closed elliptical cylindrical shell under uniform normal pressure.

In future, it would be of interest to study the deformation of noncircular cylindrical shells either of discrete-variable thickness or reinforced with ribs taking into account the nonlinear properties of a material and features of their deformation [5, 6, 8, 9].

REFERENCES

1. Ya. M. Grigorenko, V. D. Budak, and O. Ya. Grigorenko, *Solution of Shell Problems Based on Discrete-Continuum Methods* [in Ukrainian], Ilion, Nikolaev (2010).
2. Yu. Yu. Abrosov, V. A. Maksimyuk, and I. S. Chernyshenko, "Influence of cross-sectional ellipticity on the deformation of a long cylindrical shell," *Int. Appl. Mech.*, **52**, No. 5, 529–534 (2016).
3. Y. N. Chen and J. Kempner, "Buckling of oval cylindrical shell under compression and asymmetric bending," *AIAA J.*, **14**, No. 9, 1235–1240 (1976).
4. Ya. M. Grigorenko and L. V. Kharitonova, "Deformation of flexible noncircular cylindrical shells under concurrent loads of two types," *Int. Appl. Mech.*, **43**, No. 7, 754–760 (2007).
5. A. N. Guz, E. A. Storozhuk, and I. S. Chernyshenko, "Nonlinear two-dimensional static problems for thin shells with reinforced curvilinear holes," *Int. Appl. Mech.*, **45**, No. 12, 1269–1300 (2009).
6. V. Karpov and A. Semenov, "Strength and stability of orthotropic shells," *World. Appl. Sci. J.*, **30**, No. 5, 617–623 (2014).
7. T. A. Kiseleva, Yu. V. Klochkov, and A. P. Nikolaev, "Comparison of scalar and vector FEM forms in the case of an elliptic cylinder," *J. Comput. Math. Phys.*, **55**, No. 3, 422–431 (2015).
8. I. V. Lutskaya, V. A. Maximyuk, E. A. Storozhuk, and I. S. Chernyshenko, "Nonlinear elastic deformation of thin composite shells of discretely variable thickness," *Int. Appl. Mech.*, **52**, No. 6, 616–623 (2016).
9. V. A. Maximyuk, E. A. Storozhuk, and I. S. Chernyshenko, "Stress–strain state of flexible orthotropic cylindrical shells with a reinforced circular hole," *Int. Appl. Mech.*, **51**, No. 4, 425–433 (2015).
10. F. Romano and D. Ramlet, "Noncircular rings under shear load," *J. Frank. Inst.*, **284**, No. 5, 283–299 (1967).
11. K. P. Soldatos, "Mechanics of cylindrical shells with non-circular cross-section: a survey," *Appl. Mech. Rev.*, **52**, No. 8, 237–274 (1999).
12. E. A. Storozhuk and A. V. Yatsura, "Exact solutions of boundary-value problems for noncircular cylindrical shells," *Int. Appl. Mech.*, **52**, No. 4, 386–397 (2016).
13. R. C. Tennyson, M. Booton, and R. D. Caswell, "Buckling of imperfect elliptical cylindrical shells under axial compression," *AIAA J.*, **9**, No. 2, 250–255 (1971).
14. S. P. Timoshenko, *Strength of Materials, Part 2. Advanced Theory and Problems*, D. Van Nostrand Company, New York (1941).
15. F. Tornabene, N. Fantuzzi, M. Baccocchi, and R. Dimitri, "Free vibrations of composite oval and elliptic cylinders by the generalized differential quadrature method," *Thin-Walled Struct.*, **97**, 114–129 (2015).
16. G. Yamada, T. Irie, and Y. Tagawa, "Free vibration of non-circular cylindrical shells with variable circumferential profile," *J. Sound Vibr.*, **95**, No. 1, 117–126 (1984).
17. W. C. Young and R. G. Budynas, *Roark's Formulas for Stress and Strain*, McGraw-Hill, New York (2002).
18. L. P. Zheleznov, V. V. Kabanov, and D. V. Boiko, "Nonlinear deformation and stability of oval cylindrical shells under pure bending and internal pressure," *J. Appl. Mech. Tech. Phys.*, **47**, No. 3, 406–411 (2006).